Paper prepared for the Fourth US -Japan Workshop on Performance-Based Engineering for R/C Building Structures, Toba, Japan, October 22-24, 2002

Shear Failure Mechanism of Precast Prestressed Concrete Beam-Column Joints Assembled by Post-tensioning Steel Bars

KITAYAMA Kazuhiro [*1], KISHIDA Shinji [*2] and MORIYAMA Kensaku [*3]

ABSTRACT

Prestressed concrete beam-column subassemblage specimens, which were prefabricated by passing post-tensioning deformed bars through precast RC beams and column, were tested under reversed cyclic loading. Beam-column joint panel failed in shear for specimens provided bond between post-tensioning bars and concrete by grout injection, whereas concrete compressive failure due to flexural moment was observed at beam ends for unbonded specimen. To study on horizontal shear force input to joint panel, concrete compressive stress distribution acting on beam critical section was researched through measuring concrete normal strains by gauges stuck on beam surface. Central region of joint panel concrete in some height was subjected to horizontal compression by concrete stress blocks on beam critical sections on both sides of a joint. This means that all concrete compressive force at beam crtical section was not necessarily introduced to a joint panel. The joint input shear force, which was computed using measured tensile forces of post-tensioning steel bars and accounting for non-contribution of the compressive force in middle height of a joint to horizontal shear, deteriorated with the decrease in story shear force. Shear strength in interior beam-column joint obtained by above-mentioned method agreed well with shear strength predicted by AIJ provision proposed for RC beam-column joints.

1. INTRODUCTION

Shear strength in reinforced concrete (RC) beam-column joints can be obtained by Design Guidelines of Architectural Institute of Japan [1], which depends on both the joint shape such as interior, exterior or knee joint and the concrete compressive strength. Whereas, the strength in precast prestressed concrete beam-column joints assembled by post-tensioning steel bars called as PCaPC has not been estimated quantitatively. There are few tests in which joint panel failure is studied for PCaPC beam-column subassemblages [2]. Therefore PCaPC beam-column joint specimens were tested under reversed cyclic lateral loading and column axial loading to study the joint failure mechanism.

**1 Associate Professor, Graduate School of Engineering, Tokyo Metropolitan University, Dr. Eng.*
Email : kitak@ecomp.metro-u.ac.jp

**2 Research Associate, Graduate School of Engineering, Tokyo Metropolitan University, Dr. Eng.*
Email : skishida@ecomp.metro-u.ac.jp

**3 Graduate student, Tokyo Metropolitan University*
Email : moriken@ecomp.metro-u.ac.jp

Table 1 Properties of specimens

Specimens	BNU	BHH1	BHH2	BHH3
Post-tensioning Steel Bars	2-D32		2-D36	
Specified Concrete Strength of Column	60MPa		30MPa	
Column Axial Load (Compression, Stress Ratio)	937kN (0.13)		469kN (0.13)	
Mortal of Vertical Joint	Normal Strength	High Strength		
Grout	None	High Strength		
Shape of Subassemblage	Interior Beam-Column Joint			Exterior
Ratio of Initial Tensile Stress to Yield Strength of Post-tensioning Steel Bar	0.7			
Steel Factor*1	0.279			
Specified Concrete Strength of Beam	60MPa			
Column longitudinal Bars	4-D32 (SBPR 930/1080)			
Joint Lateral Bars	2-D10 2 sets			

D32 (SBPR 930/1080)：Sheath- 49mm, D36 (SBPR 930/1080)：Sheath -56mm

*1 Steel factor：$q = \frac{a_y \cdot \sigma_y + a_{py} \cdot \sigma_{py}}{bD \cdot \sigma_B}$, where, D ：depth of section,

a_y ：Section area of longitudinal steel bar, σ_y ：Yield stress of longitudinal steel bar,
a_{py} ：Section area of post-tensioning steel bar, σ_B ：Concrete compressive strength
σ_{py} ：Yield stress of post-tensioning steel bar, b ：Width of section

Table 2 Material properties of joint mortal

Joint Mortal		Compressive Strength, MPa	Secant Modulus, GPa	Tensile Strength, MPa
Normal	BNU	64.9	22.0	4.37
High	BHH1	105.3	39.1	4.07
	BHH2	101.8	37.0	4.07
	BHH3	100.1	36.1	4.07

Table 3 Material properties of grout

Grout		Compressive Strength, MPa	Secant Modulus, GPa	Tensile Strength, MPa
-	BNU	-	-	-
High	BHH1	118.3	32.5	4.91
	BHH2	112.0	31.9	4.91
	BHH3	109.2	31.6	4.91

Table 4 Material properties of steel bars

Diameter		Yield Strength, MPa	Young's Modulus, GPa	Yield Strain, %
D32	BNU	1014.4	195.1	0.720*1
	BHH1			
D36	BHH2	1023.6	211.1	0.685*1
	BHH3			
Column Longitudinal Bar (D32)		1014.4	195.1	0.720*1
Beam Longitudinal Bar (D13)		396.4	184.4	0.226
Reinforcing Bar (D10)		418.7	187.0	0.225

*1 Yield strain was determined nominally by 0.2% offset method.

Table 5 Material properties of concrete

Specimens	Compressive Strength, MPa	Strain at Maximum Strength, %	Secant Modulus, GPa	Tensile Strength, MPa
BNU	76.6	0.258	41.1	4.45
BHH1	77.2	0.260	41.1	
BHH2*1	43.0	0.216	33.1	2.99
	71.7	0.255	39.7	4.45
BHH3*1	39.9	0.212	32.2	2.99
	67.4	0.257	38.0	4.45

*1 Upper column:concrete of column , Lower column: concrete of beam

2. OUTLINE OF TEST

2.1 SPECIMENS

Properties of specimens are summarized in Table 1. Section dimensions and reinforcement

details are shown in Fig.1. Three plane cruciform and one exterior beam-column joint specimens with two-fifth scale to actual frames were tested. Beam and column elements were precast separately. Post-tensioning steel bars with deformed surface were used to connect precast RC beams and column for all specimens. Therefore beam longitudinal bars were terminated at column face without passing through a beam-column joint panel. The gap with the width of 20 mm between precast beam and column was filled with normal or high strength mortal. Bond along post-tensioning steel bars was provided by injecting high strength grout mortal into the sheath except for Specimen BNU. Unbonded post-tensioning steel bars were used for Specimen BNU. The column section was square with 350mm depth. The depth and width of a beam section were 400mm and 250mm, respectively. Two sets of 2-D10 were arranged in a beam-column joint region as the lateral reinforcement for all specimens. The length from the center of column to the pin-roller support of beam end was1600mm. The height from the center of beam to the loading point on the top of the column or to the bottom support was 1415mm. The shear span ratio was 4.0 in the column and 4.3 in the beam, respectively.

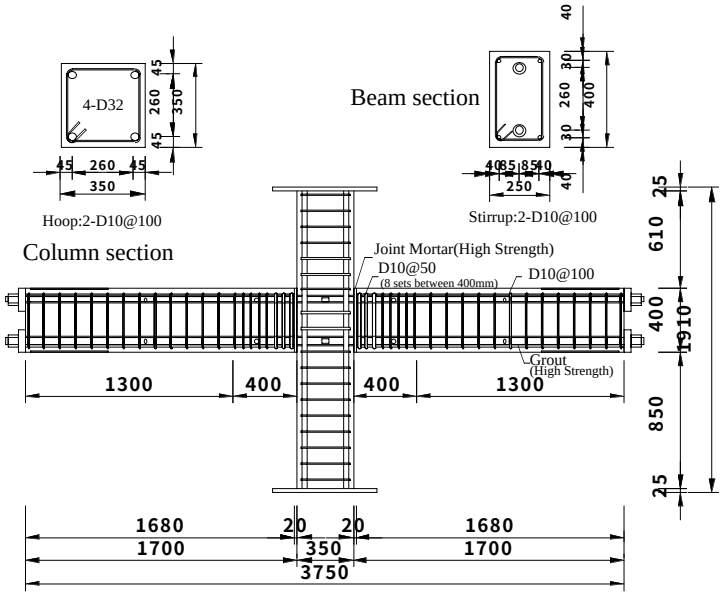

Fig. 1 Section dimensions and reinforcement details

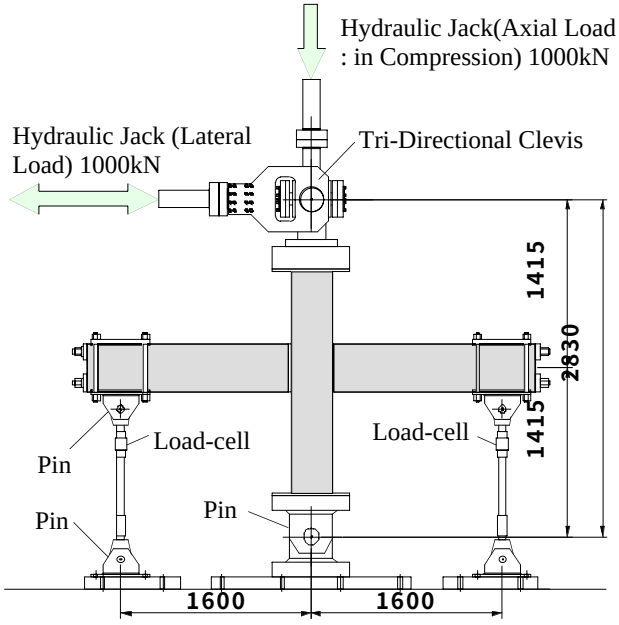

Fig. 2 Loading apparatus

Specimens BNU and BHH1 were designed to develop beam yielding. Concrete compressive strength of 30MPa for a column and the diameter of 36mm for a post-tensioning steel bar were chosen to cause joint shear failure for Specimens BHH2 and BHH3. The amount of the stirrup in beam hinge regions was increased to two times more than that in elastic region. Specimen BHH3 is the exterior beam-column joint. The post-tensioning steel beam

bars were anchored with the anchor plates outside the column face. Material properties of concrete, mortal, grout and steel are listed in Tables 2,3,4 and 5.

2.2 LOADING METHOD AND INSTRUMENTATION

The loading system is shown in Fig.2. The beam ends were supported by horizontal rollers, while the bottom of the column was supported by a mechanical hinge. The reversed horizontal load and the constant axial load in compression were applied at the top of the column. All Specimens were controlled by the story drift angle for one cycle of 1/400, two cycles of 1/200 and 1/100, one cycle of 1/66, two cycles of 1/50, one cycle of 1/33 and two cycles of 1/25. Lateral force applied to the top of a column, column axial load and shear forces of both beam ends were measured by load-cells. Story drift, beam and column deflections, and local displacement of a joint panel were measured by displacement transducers. Strains of prestressing steel bars, beam bars, column bars and the joint lateral reinforcement were measured by strain gauges. Moreover, concrete strain distribution at the beam end adjacent to column face was measured by concrete strain gauges stuck on concrete surface (see Fig.7).

3. TEST RESULTS

3.1 CRACK PATTERNS AND FAILURE MODE

Crack patterns at the end of test are shown in Fig.3. Flexural cracks in beams and column and diagonal shear cracks in a joint panel were observed for all specimens. The column longitudinal bars did not yield. Joint lateral reinforcement yielded for all specimens. Post-tensioning steel bars passing through beams yielded for Specimen BHH1. On the contrary, for other specimens post-tensioning steel bars of the beam did not yield. Diagonal joint shear cracks expanded considerably. The shell concrete spalled off in a joint panel except for Specimen BNU. The diagonal shear cracks were not observed in beams for all specimens. Concrete compressive failure at beam ends occurred for Specimen BNU without diagonal crack opening in a joint panel. It was concluded that Specimens BHH2 and BHH3 failed in joint shear, Specimen BNU failed by concrete compression at beam ends due to bending moment and Specimen BHH1 failed eventually in joint shear after the post-tensioning steel bars yielded.

3.2 STORY SHEAR - DRIFT RELATIONSHIP

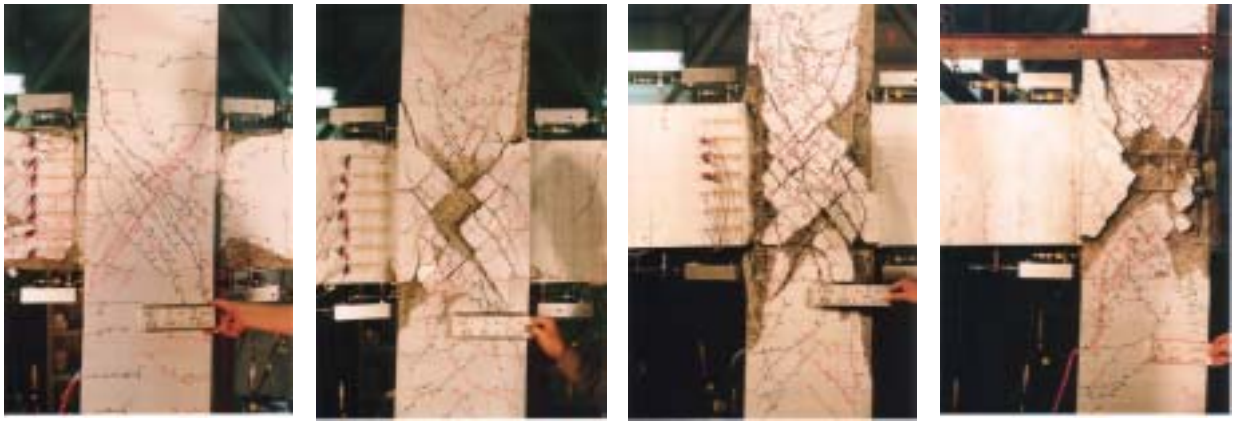

(a) Specimen BNU (b) Specimen BHH1 (c) Specimen BHH2 (d) Specimen BHH3

Fig. 3 Crack patterns at end of test

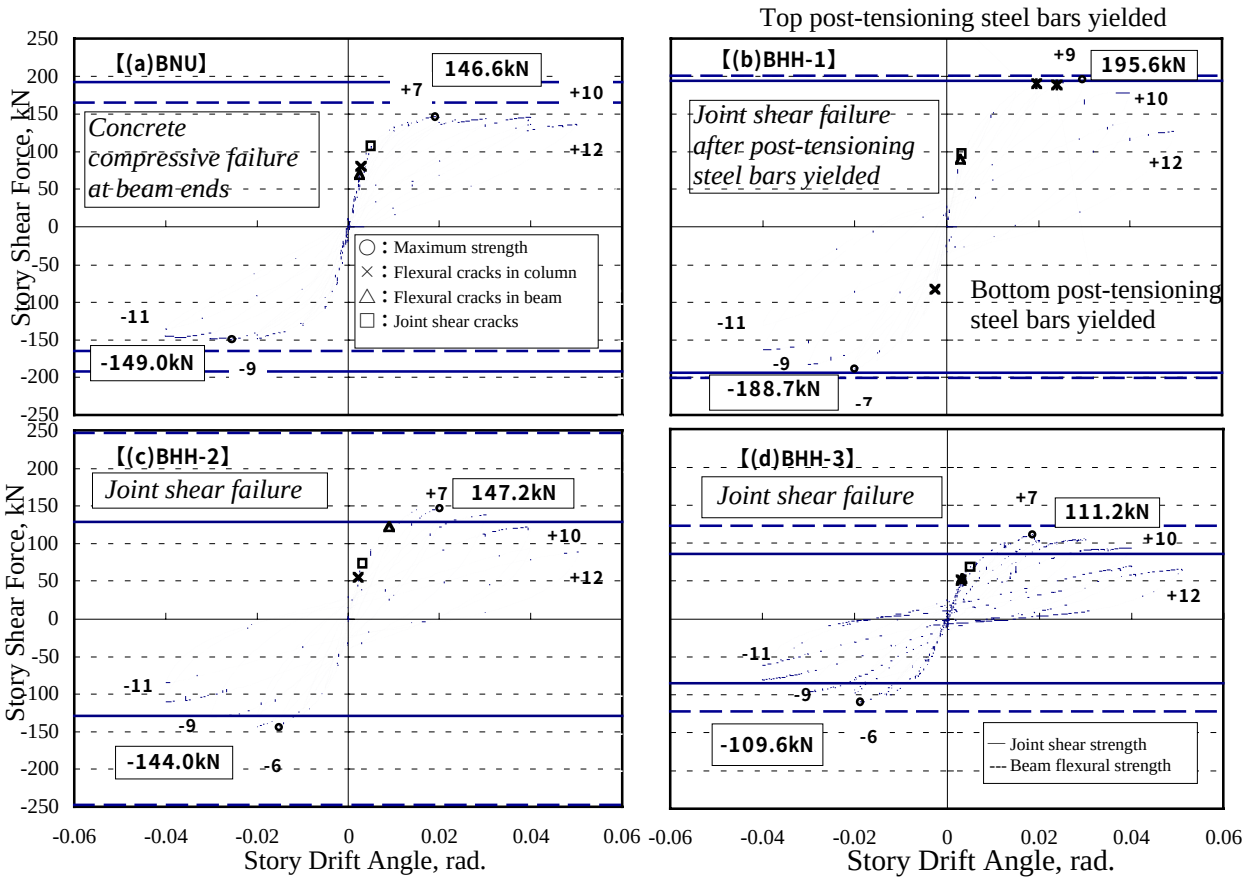

Fig. 4 Story shear - drift relations

The story shear force - story drift relationships are shown in Fig.4. The story shear force was computed from moment equilibrium between measured beam shear forces and the horizontal force at the loading point on the top of the column. The occurrence of flexural cracking in beams and column, diagonal shear cracking in a joint panel and yielding of post-tensioning steel bars are marked in Fig.4. The joint shear strength computed according to Architectural Institute of Japan (AIJ)[1] and beam flexural strength are shown by a solid

line and a dotted line respectively in Fig.4. The lever arm lengths in beam and column section were assumed to be 289mm and 267mm respectively when joint shear strength was converted to corresponding story shear force. Beam flexural strength was calculated by the section analysis on the basis of the assumption that plane sections remain plane. The story shear reached the maximum force at the story drift angle of 1.5% for Specimen BHH3, 2% for Specimen BHH2 and 3% for Specimens BNU and BHH1. The measured maximum story shear for Specimens BHH2 and BHH3 was larger than the calculated nominal strength, whereas that for other two specimens was smaller than the calculated strength. The story shear force decreased gradually after story shear force reached the maximum value.

3.3 DISPLACEMENT CONTRIBUTION

The contribution of deformation of beams, column and joint panel to the story drift was calculated and shown in Fig.5. The horizontal axis represents the measured story drift. Total of each components did not always correspond with the directly measured story drift, including a little tolerance to use the measured value for each components. The beam-column joint panel deformation was large from the start of test and increased until the story drift angle of 3% for Specimens BHH2 and BHH3. The beam deformation shared more than 60 percent of the total story drift for Specimen BNU. The beam-column joint panel deformation for Specimen BHH1 increased radically after the story drift angle of 3% at which damage of concrete in a joint panel became severe and post-tensioning steel bars yielded.

4. DISCUSSIONS

The stresses of post-tensioning steel bars used in the paper were obtained from strains

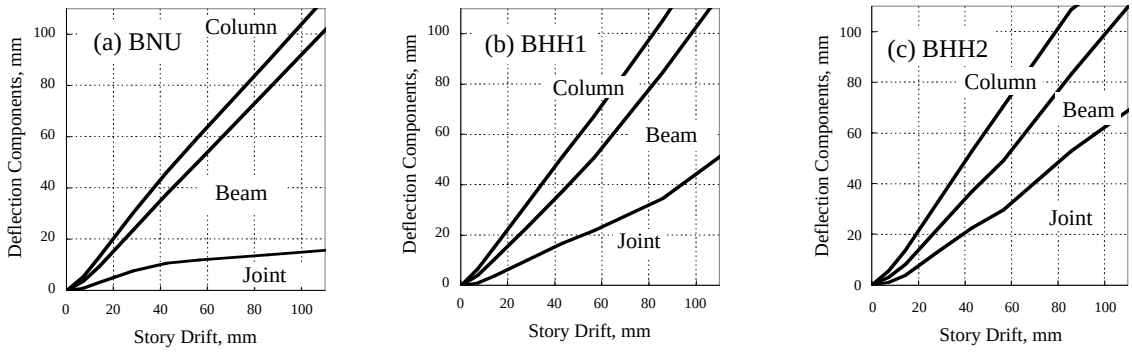

(a) Concrete compressive failure at beam ends

(b) Joint shear failure after yielding of post-tensioning steel bars

(c) Joint shear failure

Fig. 5 Deflection components to story drift

measured by strain gauges through hexa-linear stress - strain relationship model as shown in Fig.6, where stress of the deformed post-tensioning steel bar with the diameter of 32mm was traced as a instance with measured strain.

4.1 COMPARISON BETWEEN MEASURED AND COMPUTED STORY SHEAR

The comparisons between test results and calculations are shown in Table 6. Diagonal shear crack strength in a joint panel (τ_{cr}) was obtained by Equation (1) based on the principal stress field taking account of the prestress to a beam (σ_p :σ_p < 0) and the axial compressive stress to a column(σ_o : σ_o< 0).

$$\tau_{cr} = \sqrt{f_t^2 - f_t(\sigma_o + \sigma_p) + \sigma_o \cdot \sigma_p} \qquad (1)$$

where f_t is a concrete tensile strength. Compressive stress σ_p was obtained by dividing initial prestress force to a beam by the product of column width and beam depth. Measured joint shear stress was computed from Equations (2) or (3) assuming that joint shear resistant area is the product of column depth and the average of beam and column width. Measured joint shear stress at joint diagonal crack was smaller than computed crack strength for all specimens since uniform compressive stress field as supposed in Equation (1) was not formed in a joint panel due to separation between beam and column at beam critical sections.

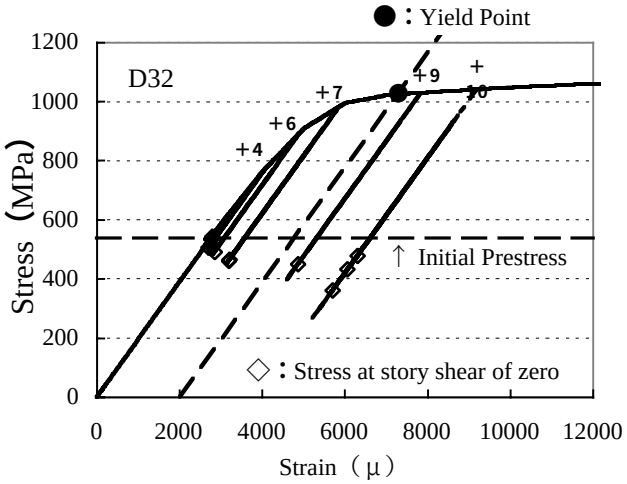

Fig. 6 Hexa-linear stress-strain model

Table 6 Test results

Specimen	BNU	BHH1	BHH2	BHH3
Measured Story Shear Force at Joint Shear Crack (kN)	107	97	74	69
Measured Story Shear Strength at Positive Loading (kN)	147	196	147	111
Corresponding Story Drift Angle (rad.)	0.02	0.03	0.02	0.015
Measured Story Shear Strength at Negative Loading (kN)	149	189	144	110
Corresponding Story Drift Angle (rad.)	0.03	0.02	0.015	0.015
* Measured Joint Shear stress at Joint Shear Crack (MPa)	7.8	7.7	6.9	5.2
** Computed Joint Shear Crack Strength (MPa)	11.1	11.0	8.3	8.3
* Measured Maximum Joint Shear stress (MPa)	10.2	14.4	12.6	8.6
*** Computed Joint Shear Strength (MPa)	17.6	17.7	11.6	8.3

* Joint shear force was obtained by Eqs. (2) or (3).
**Joint shear crack strength computed according to Reference[4]
*** Average joint shear strength computed according to Reference[1]

4.2 TRANSITION OF NEUTRAL AXIS DEPTH

Concrete strain gauges as shown in Fig.7 were stuck on the surface of a beam at the location of 60 mm apart from a beam critical section. Change of the neutral axis position

on a beam critical section was investigated by using concrete strain distribution. Method for deciding the beam neutral axis position is explained for example by Fig.8. Measured compressive strain distribution at the locations of C1 from C4, excluding tensile strains at the locations of C5 from C7, was approximated by the line induced from least squares method. Hence the neutral axis position was decided as the point at which obtained strain line crosses the vertical axis of zero strain. The shape of concrete compressive stress block can be assumed as triangle as shown in Fig.8.

Transitions of the neutral axis position are shown in Fig.9 for all specimens. The neutral axis depth for Specimens BHH2 and BHH3 which failed in joint shear was greater than the half of beam depth, i.e., 200 mm, during tests. In other words central region of joint panel concrete in some height was subjected to horizontal compression by concrete stress blocks on beam critical sections on both sides of a joint as shown in Fig.11 (b). This means that all concrete compressive force at beam crtical section was not necessarily introduced to a joint panel as a horizontal shear. This is investigated quantitatively in next section.

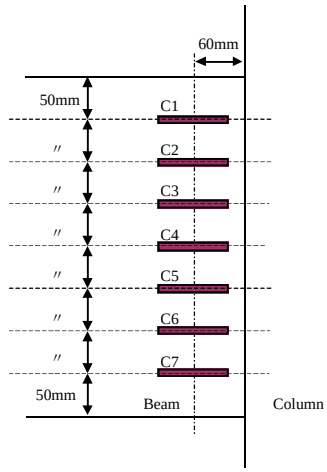

Fig. 7 Location of concrete srain gauges on beam surface

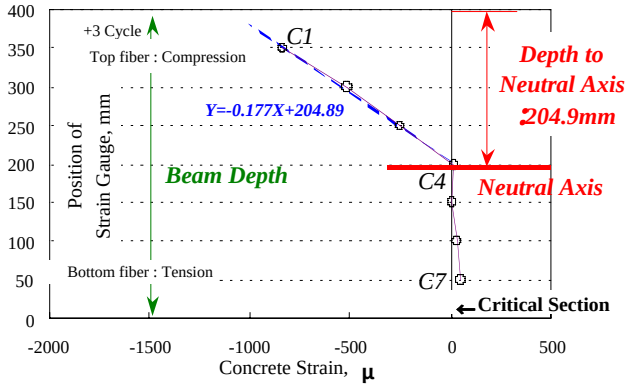

Fig. 8 Determination for beam neutral axis depth

4.3 JOINT INPUT SHEAR FORCE

Envelope curves of relationship between joint shear stress and shear distortion are shown in Fig.10. The joint shear average strength calculated according to AIJ provisions [1] is also shown by a solid line. Joint input shear force denoted as V_{jh} was computed by Equations (2) or (3) according to the definition shown in Fig.11. As mentioned in Section 4.2, it is necessary to consider two cases which one is 1) that the distance from the extreme compression fiber to neutral axis (depth of compressive stress distribution) is less than the half of beam depth as illustrated in Fig.11 (a), the other is 2) that it is greater than the half of

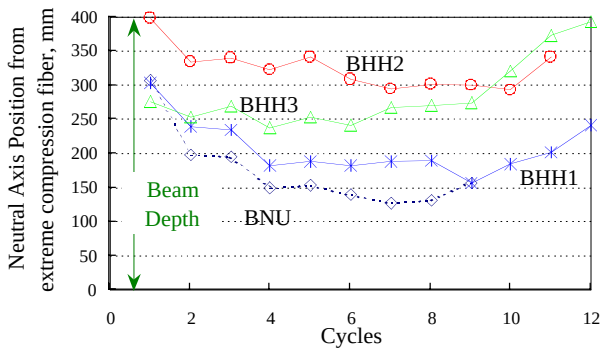

Fig. 9 Transition of beam neutral axis depth

beam depth as illustrated in Fig.11 (b). In the second case, the maximum joint shear force can be obtained mathematically along horizontal section at the center of joint depth. Therefore joint input shear force was computed as Equation (3).

1) In case that depth of compressive stress block is less than the half of beam depth;

$$V_{jh} = P_{t1} + P_{b2} - V_c \qquad (2)$$

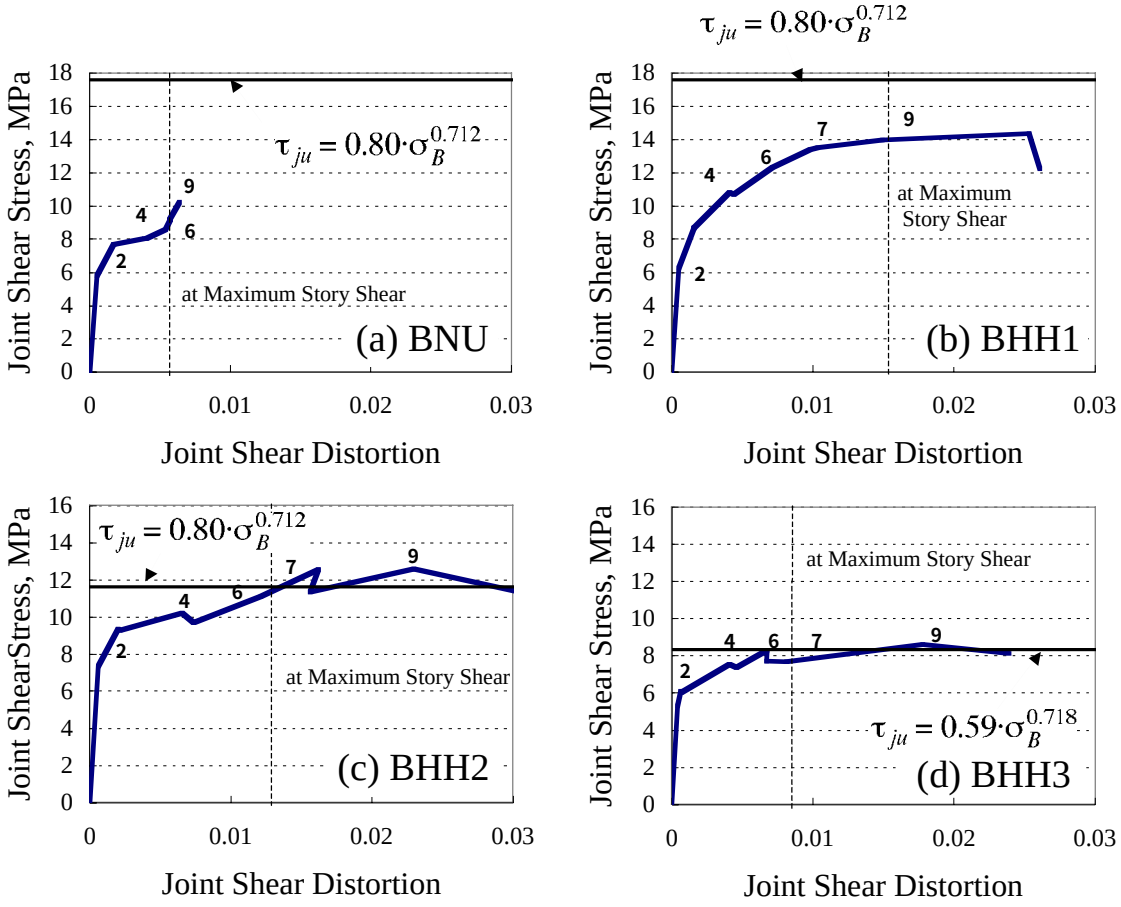

Fig. 10 Joint shear stress - shear distortion relations

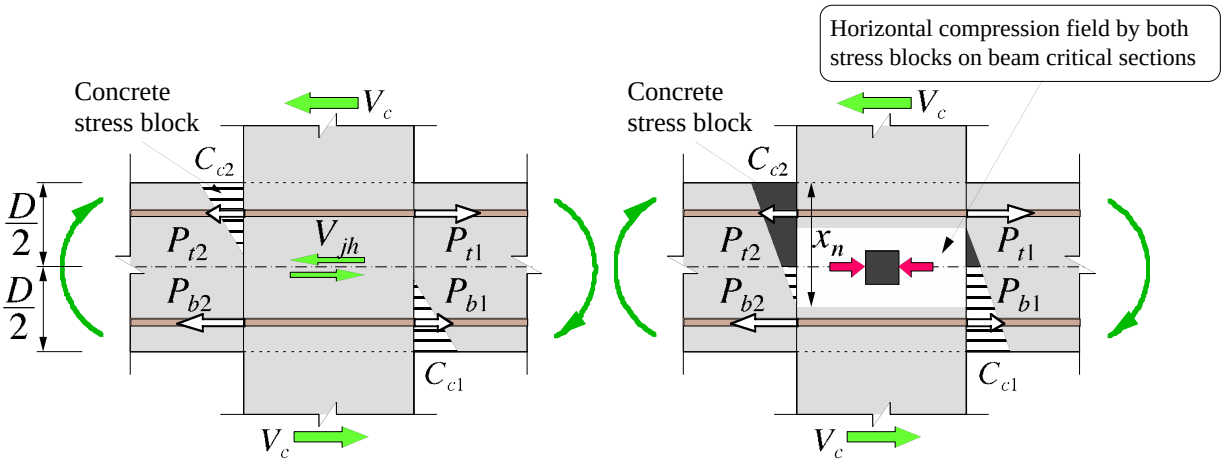

(a) In case that depth of concrete stress block is less than half of beam depth

(b) In case that depth of concrete stress block is greater than half of beam depth

Fig. 11 Stress acting on joint panel

2) In case that depth of compressive stress block denoted as x_n in Fig.11 (b) is greater than the half of beam depth;

$$V_{jh} = \alpha_1 C_{c2} - P_{t2} + P_{t1} - \alpha_2 C_{c1} - V_c \quad (3)$$

$$C_{c1} = P_{t1} + P_{b1} \quad (4)$$

$$C_{c2} = P_{t2} + P_{b2} \quad (5)$$

$$\alpha_1 = 1 - \alpha_2 \quad (6)$$

$$\alpha_2 = \frac{\left(x_n - \frac{D}{2}\right)^2}{x_n^2} \quad (7)$$

where P_{t1} and P_{t2} are measured tensile forces of the top post-tensioning steel bar, P_{b1} and P_{b2} are measured tensile forces of the bottom post-tensioning steel bar, C_{c1} and C_{c2} are concrete compressive resultant forces and V_c is measured story shear force.

Joint shear strength for Specimens BHH2 and BHH3 which was computed by Equation (3) agreed well with average strength predicted by AIJ provisions [1]. For these specimens failed in joint panel, joint shear force reached the strength at the joint shear distortion of 2% approximately after story shear force attained the maximum. For Specimen BNU which failed by concrete flexural compression at beam ends, joint shear force continued to increase even during keeping story shear force almost constant.

Equation (2) is used customarily for taking joint input shear force. Therefore joint input shear forces computed by Equations (2) and (3) were compared in Fig.12 for Specimen BHH2. Solid line shows shear force computed by Equation (2) and dotted line by Equation (3). The joint shear force calculated by customary method, i.e., Equation (2) was 1.1 times greater than that calculated by Equation (3). It is noted that the overlapping of concrete stress blocks across a joint panel on opposite beam critical sections should be considered when joint input shear force is computed in tests.

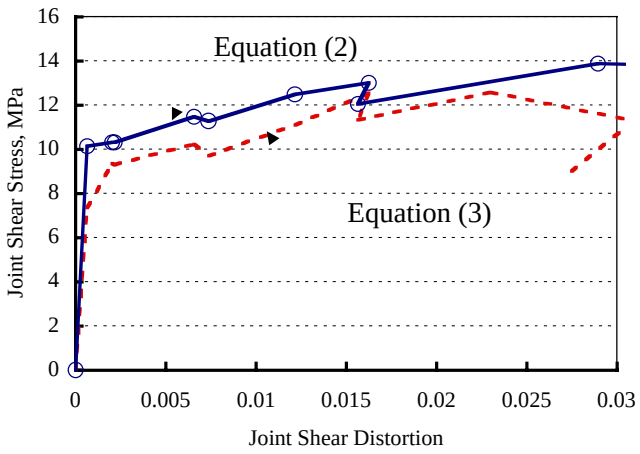

Fig. 12 Difference of joint shear stress between two computing methods

4.4 LOCATION OF COMPRESSIVE RESULTANT FORCE ON BEAM CRITICAL SECTION

With the aim of understanding the stress state around beam-column joint panel, the position of the concrete compressive resultant force on a beam critical section was computed using tensile forces of post-tensioning steel bars and beam bending moment calculated from measured beam shear. The transition of location of compressive resultant forces, tensile resultant forces and lever arm length are shown in Fig13. The specific examples at the story drift angle of 2% are shown in Fig.14. Compressive resultant force was located between top post-tensioning steel bar and the extreme compression fiber for all specimens. The lever

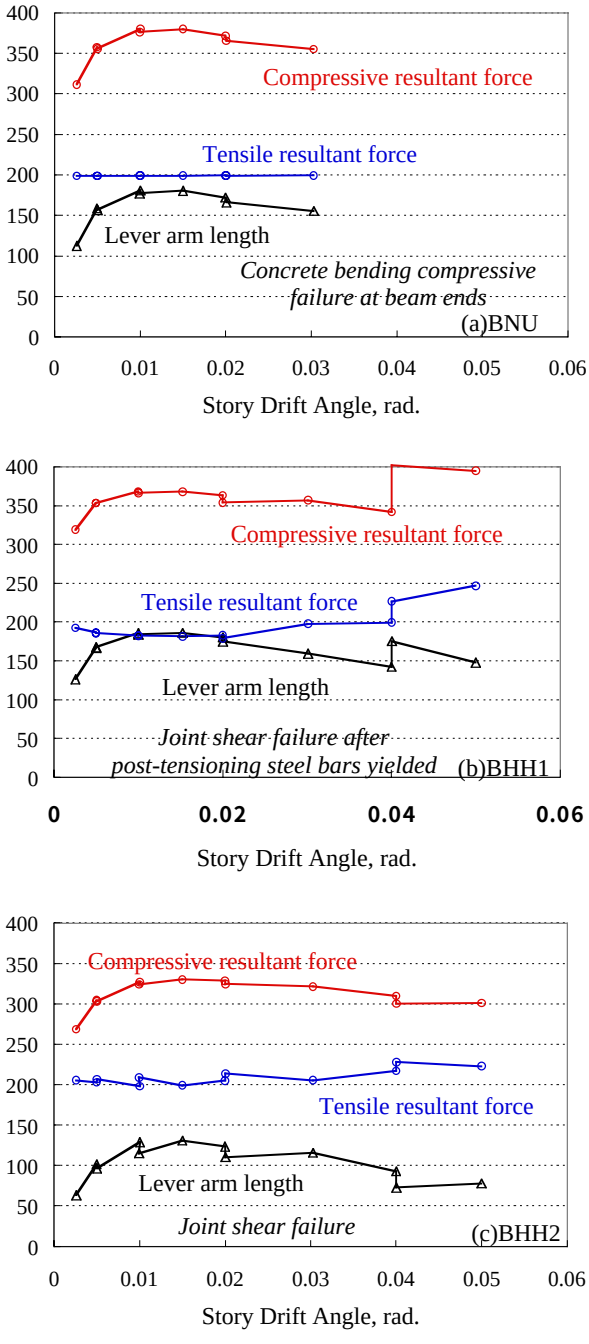

Fig. 13 Transition of location of compressive, tensile resultant forces and lever arm length on beam critical section

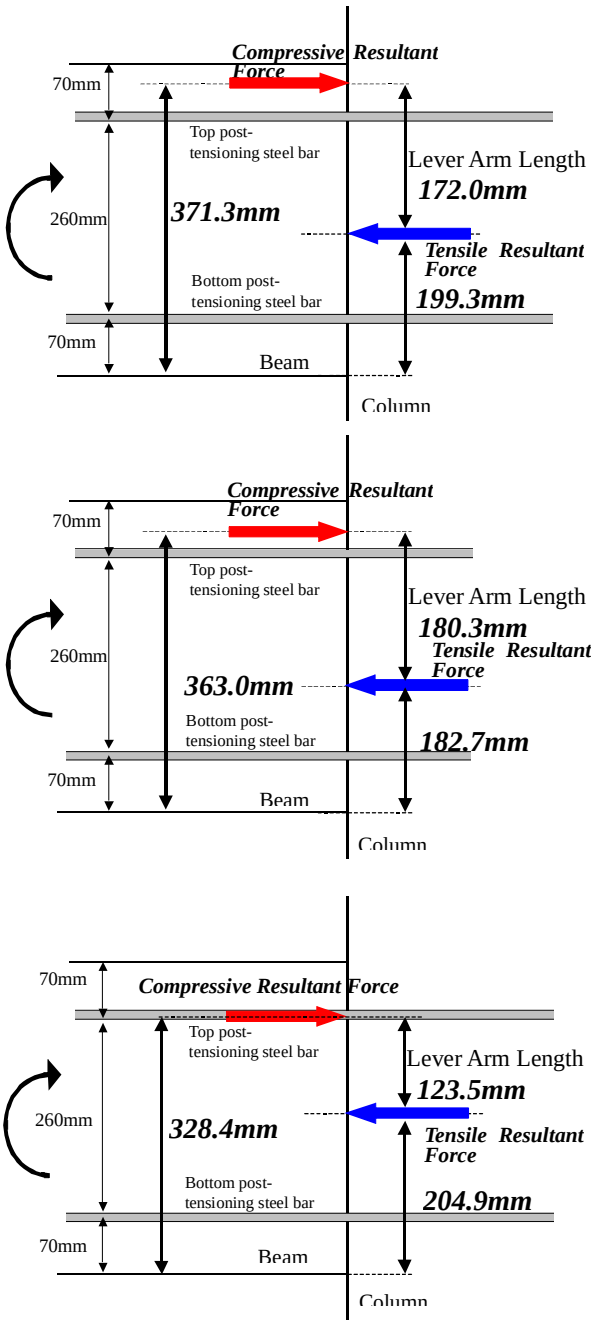

Fig. 14 Location of compressive, tensile resultant forces and lever arm length at story drift angle of 2 %

arm lengths changed from 0.3d to 0.6d (d : 330mm).

Lever arm length on prestressed beam section was shorter than that on general RC sections because the tensile resultant force of top and bottom post-tensioning steel bars was located near the center of beam section during a test.

The reason why the story shear force declined after the strength is that tensile resultant force was kept constant after the post-tensioning steel bars yielded, wheras the lever arm length gradually decreased as shown in Fig.13.

4.5 BOND ALONG BEAM POST-TENSIONING STEEL BARS

The average bond stresses along a beam post-tensioning steel bars within a joint for all specimens are shown in Fig.15. The average bond stress was computed by the difference between beam post-tensioning steel bar forces at opposite column faces. Bond stress of 1 MPa for Specimen BHH2 was kept to the story drift angle of 1.5% and decreased whereas the tensile force of beam post-tensioning steel bars at critical sections increased to the story drift angle of 3.0%. It is judged that the decrease in bond stress along beam post-tensioning steel bars within a joint panel resulted from bond deterioration. Bond strength for Specimen BHH1 was greater than that for other specimens since high strength concrete was cast for the column. The bond deteriorated before the story shear force reached the maximum for all specimens.

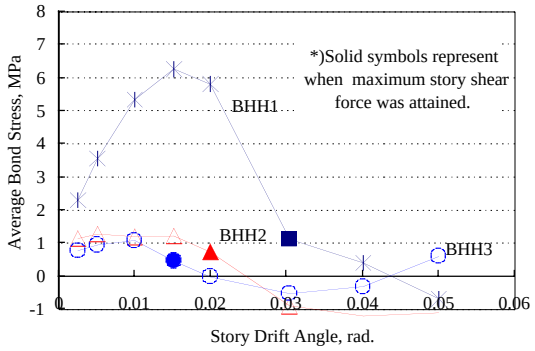

Fig. 15 Average bond stress along beam post-tensioning steel bar within joint

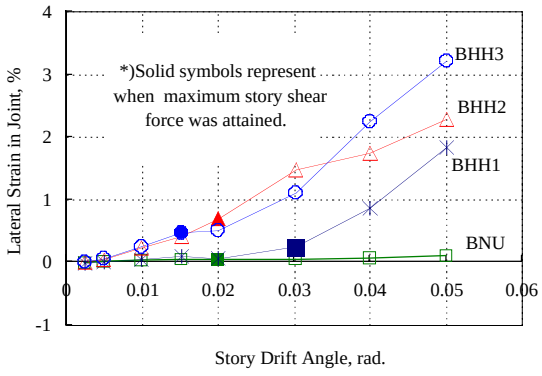

Fig. 16 Lateral strain in joint panel

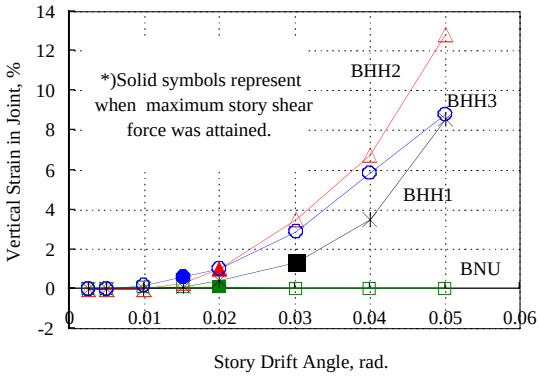

Fig. 17 Vertical strain in joint panel

4.6 DEFORMATION OF JOINT PANEL

The lateral and vertical average strains in a joint panel are shown in Figs.16 and 17,

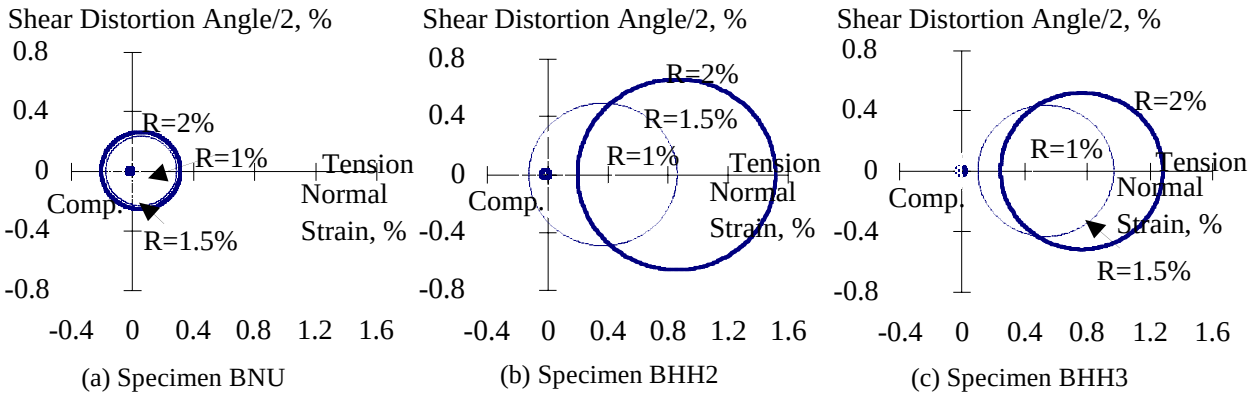

Fig. 18 Mohr's strain circles for joint panel

respectively. These strains were computed by using average displacements measured by two horizontal and vertical displacement transducers. Both lateral and vertical average tensile strains kept increasing after the story shear force reached the maximum for all specimens. Both average strains were negligible for Specimen BNU, which did not fail in joint shear.

Mohr's strain circles are shown in Fig.18 to the story drift angle of 2% to investigate deformation characteristics of a joint panel in more detail. The larger Mohr's circle is, the severer the damage in a joint panel is. The strain circles of Specimens BHH2 and BHH3 which failed in joint shear were larger than that for Specimen BNU. Centers of circle shifted largely to the tensile side. This indicates that the joint panel concrete expanded isotropically with the increase in a story drift. Joint shear failure for both specimens was caused by the concrete expansion.

The strain circle for Specimen BNU that did not fail in joint shear was small. Center of circle was located at the origin and the Mohr's strain circle became large like as concentric circles.

5. CONCLUSIONS

The following conclusions can be drawn from the present study:

(1) Interior and exterior beam-column joints which were made of assembling precast RC beams and column through post-tensioning steel bars failed in shear.

(2) The depth of compressive stress block computed by the concrete strains at beam critical section was larger than the half of beam depth. This indicates that joint panel concrete in central

height was subjected to horizontal compression by concrete stress blocks on beam critical sections on both sides of a joint. Therefore all concrete compressive force on beam critical section did not necessarily contribute to joint input shear.

(3) The joint input shear force was computed by using the measured tensile forces of post-tensioning steel bars and considering that two concrete compressive stress blocks on opposite beam critical sections of a joint panel overlapped as mentioned above.

(a) Joint shear force reduced with the decrease in story shear force after the joint panel failed by shear.

(b) Shear strength of PCaPC beam-column joints can be estimated by the prediction formula for usual RC beam-column joints.

(4) Joint failure was caused by the expansion of joint core concrete.

ACKNOWLEDGMENT

The authors would like to thank Dr. MARUTA Makoto and Ms. KIMURA Akiko, research engineers in Kajima Technical Research Instiute, for their cooperative works.

REFERENCES

[1] Architectural Institute of Japan : Design Guideline for Earthquake Resistant Reinforced Concrete Buildings Based on Inelastic Displacement Concept,1999, (in Japanese).

[2] Beniya, N., T. Kashiwazaki and H. Noguchi : An Experimental Study on Shear Behavior of Prestressed Concrete Beam-Column Connection, *Proceedings of the Japan Concrete Institute*, Vol.19, No.2, pp.1179-1184, 1997, (in Japanese).

[3] Architectural Institute of Japan : Standard for Structural Design and Construction of Prestressed Concrete Structures,1998, (in Japanese).

[4] Architectural Institute of Japan : Design Method of Prestressed (Reinforced) Concrete Structural Members -Actual Situation and Future, 2000.4, (in Japanese).